# Unfolding Nonlinear Dynamics in Analogue Systems With Mem-Elements

Mauro Di Marco, Mauro Forti, Fernando Corinto, *Senior Member, IEEE*, and Leon Chua, *Life Fellow, IEEE*

***Abstract*— The paper considers a relevant class of networks containing memristors and (possibly) nonlinear capacitors and inductors. The goal is to unfold the nonlinear dynamics of these networks by highlighting some main features that are potentially useful for real-time signal processing and in-memory computing. In particular, an analytic treatment is provided for dynamic phenomena as the presence of invariant manifolds, the coexistence of different regimes, complex dynamics and attractors and the phenomenon of bifurcations without parameters, i.e., bifurcations due to changing the initial conditions of the state variables for a fixed set of circuit parameters. The paper also addresses the issue of how to design pulse independent voltage or current sources to steer the network dynamics through different manifolds and attractors. Two relevant examples are worked out in details, namely, a variant of Chua's circuit with a memristor and a nonlinear capacitor and a relaxation oscillator with a memristor and a nonlinear inductor. In the latter example, the paper also studies the effect on manifolds and coexisting dynamics when real memristive devices are accounted for using a class of extended memristor models. The analysis is conducted by means of a recently developed technique named flux-charge analysis method (FCAM). Numerical simulations are presented to confirm the theoretic findings.**

***Index Terms*— Bifurcations without parameters, coexisting attractors, complex dynamics, flux-charge analysis, invariant manifolds, memristor, nonlinear inductors and capacitors.**

## I. Introduction

CONVENTIONAL computing architectures are facing fundamental challenges including the heat and memory wall, the end of Moore's law and the von Neumann bottleneck, i.e., the high (energy and speed) costs associated with constant data movements between the memory and the processor [1], [2]. Memristor and, more generally, mem-element technology, offers itself as a promising one to fill the gap of Moore's law by enabling high-efficient on-chip memory storage, bioinspired computing and the possibility to implement efficient reconfigurable in-memory computing systems [3]–[6].

A deep understanding of the nonlinear dynamics of mem-circuits is essential to exploit them for analogue signal processing purposes [7]–[13]. Recent papers [14]–[16] have developed a technique, named Flux-Charge Analysis Method (FCAM), to effectively analyze and uncover the peculiar dynamical properties of networks with mem-elements. FCAM has been used so far to analyze some relevant classes of mem-networks as those containing memristors, memcapacitors, meminductors together with *linear* capacitors and inductors [4], [15], [16]. For modeling purposes at nanoscale, mem-elements are sometimes used in combination with *nonlinear* inductors or capacitors. This is true for instance for the classical circuit model for a Josephson junction, that consists of a parallel connection of a linear capacitor, a linear resistor, and a nonlinear flux-controlled inductor. A more rigorous quantum mechanical analysis of the Josephson junction dynamics reveals the presence of an additional current component due to interference among quasi-particle pairs, which can be modeled with the current flowing into a flux-controlled memristor [17].

In the paper, a class $\mathcal{N}$ of mem-circuits containing any number of memristors and (possibly) *nonlinear* capacitors and inductors, is considered. The goal is to extend FCAM in order to unfold the nonlinear dynamics of networks in $\mathcal{N}$ by highlighting some main peculiar features that are potentially useful for real-time signal processing and in-memory computing. The main contributions in the paper consist of an analytic treatment of the following dynamic phenomena.

- *Invariant manifolds.* It is shown that the state space in the voltage-current $(v, i)$-domain can be foliated in a continuum of manifolds that are positively invariant for the dynamics in the inputless case.
- *Coexisting lower-order dynamics and attractors.* It is proved that on each manifold a circuit displays a different reduced-order dynamics and attractors.
- *Bifurcations without parameters.* Due to the presence of invariant manifolds, we can observe bifurcations due to changing the initial conditions for the state variables even if the circuit parameters are held fixed (bifurcations without parameters).
- *Programming with pulses.* We show that it is possible to steer a circuit trajectory through different manifolds,

Manuscript received April 2, 2020; revised July 31, 2020; accepted September 11, 2020. Date of publication September 22, 2020; date of current version December 21, 2020. This work was supported by the Ministero dell'Istruzione, dell'Universitá e della Ricerca (MIUR) under Contract 2017LSCR4K-003. This article was recommended by Associate Editor T. Serrano-Gotarredona. *(Corresponding author: Mauro Forti.)*

Mauro Di Marco and Mauro Forti are with the Department of Information Engineering and Mathematics, University of Siena, 53100 Siena, Italy (e-mail: dimarco@dii.unisi.it; forti@diism.unisi.it).

Fernando Corinto is with the Department of Electronics and Telecommunications, Politecnico di Torino, 10129 Torino, Italy (e-mail: fernando.corinto@polito.it).

Leon Chua is with the Department of Electrical Engineering and Computer Sciences, University of California, Berkeley, Berkeley, CA 94720 USA (e-mail: chua@berkeley.edu).

Color versions of one or more of the figures in this article are available online at https://ieeexplore.ieee.org.

Digital Object Identifier 10.1109/TCSI.2020.3024248

dynamics and attractors, by applying suitable pulse independent voltage or current sources.
- *Extension to real memristive devices.* We show via an example that the technique in the paper can be applied to some classes of circuits where (ideal) memristors are replaced by memristive devices belonging to a class of extended memristors.

The unfolding, and the main results obtained in the paper, are illustrated by means of two examples. The first one concerns a variant of Chua's circuit with a memristor and a nonlinear capacitor, for which it is shown that there is coexistence of different regimes and attractors as equilibrium points, cycles and complex attractors, for a fixed set of circuit parameters. The second one concerns a relaxation oscillator with a class of extended memristors and a nonlinear inductor, for which there is coexistence of equilibrium points and limit cycles.

## II. A Class of Circuits With Mem-Elements

Let $v(t)$ and $i(t)$ be the voltage and current, respectively, of a two-terminal element $\mathcal{D}$. The flux (or voltage momentum) is given by $\varphi(t) = \int_{-\infty}^{t} v(\tau)d\tau$, whereas the charge (or current momentum) is $q(t) = \int_{-\infty}^{t} i(\tau)d\tau$. Also define the *incremental flux* $\varphi(t;t_0) = \int_{t_0}^{t} v(\tau)d\tau$ and *incremental charge* $q(t;t_0) = \int_{t_0}^{t} i(\tau)d\tau$ at the terminals of $\mathcal{D}$, where $t \geq t_0$ and $t_0$ is a finite initial instant.

We consider henceforth a class $\mathcal{N}$ of nonlinear circuits containing:
- flux-controlled memristors, denoted by $\mathcal{D} \in \mathrm{M}_\varphi$ and defined by the constitutive relation (CR) $q_M = f_M(\varphi_M)$
- charge-controlled memristors, denoted by $\mathcal{D} \in \mathrm{M}_q$ and defined by the CR $\varphi_M = f_M(q_M)$
- possibly nonlinear charge-controlled capacitors ($\mathcal{D} \in \mathrm{C}_q$) with CR $v_C = f_C(q_C)$
- possibly nonlinear flux-controlled inductors ($\mathcal{D} \in \mathrm{L}_\varphi$) with CR $i_L = f_L(\varphi_L)$
- linear resistors $v = Ri$ and independent voltage and current sources with CR $v_e(t) = e(t)$ and $i_a(t) = a(t)$, respectively.

In the flux-charge $(\varphi, q)$-domain the CRs of the elements are given as follows:
- $\mathcal{D} \in \mathrm{M}_\varphi$:
$$q_M(t;t_0) = f_M(\varphi_M(t;t_0) + \varphi_{M0}) - f_M(\varphi_{M0})$$
where $\varphi_{M0} = \varphi_M(t_0)$
- $\mathcal{D} \in \mathrm{M}_q$:
$$\varphi_M(t;t_0) = f_M(q_M(t;t_0) + q_{M0}) - f_M(q_{M0})$$
where $q_{M0} = q_M(t_0)$
- $\mathcal{D} \in \mathrm{C}_q$:
$$\dot{\varphi}_C(t;t_0) = f_C(q_C(t;t_0) + q_{C0})$$
where $q_{C0} = q_C(t_0)$
- $\mathcal{D} \in \mathrm{L}_\varphi$:
$$\dot{q}_L(t;t_0) = f_L(\varphi_L(t;t_0) + \varphi_{L0})$$
where $\varphi_{L0} = \varphi_L(t_0)$
- linear resistors: $\varphi_R(t;t_0) = Rq_R(t;t_0)$;
independent voltage sources: $\varphi_e(t;t_0) = \int_{t_0}^{t} e(\tau)d\tau$;
independent current sources: $q_a(t;t_0) = \int_{t_0}^{t} a(\tau)d\tau$.

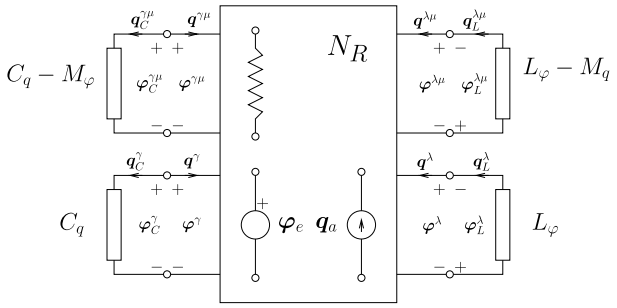


Fig. 1. Decomposition of a circuit $N \in \mathcal{N}$.

### A. State Equations in the $(\varphi, q)$-Domain

The article [18] has addressed the problem of writing a global state equation (SE) representation for a circuit $N \in \mathcal{N}$ under suitable assumptions. Next, we briefly recall some results from that paper. The SEs are then used for addressing the main topic of this paper, i.e., the unfolding of the dynamics of circuits in the class $\mathcal{N}$.

Consider a circuit $N \in \mathcal{N}$. In the $(\varphi, q)$-domain, $N$ satisfies Kirchhoff charge law (K$q$L) and Kirchhoff flux law (K$\varphi$L) for incremental charges and fluxes [14]. Taking into account also the CRs of the elements $\mathcal{D} \in N$, it is seen that a circuit $N \in \mathcal{N}$ in the $(\varphi, q)$-domain is analogous to a nonlinear $RLC$ circuit described in the $(v, i)$-domain. Based on this analogy, we can tackle the problem of writing the SEs of $N$ using well established results for nonlinear $RLC$ circuits [19].

To find the SE representation in the $(\varphi, q)$-domain, it is convenient to represent a circuit $N \in \mathcal{N}$ as a resistive multi-port $N_R$ containing the linear resistors and flux and charge sources terminated by a number of two-terminal elements. The hybrid description of $N_R$ [20] is then used for writing the SEs. In particular, we assume that $N$ is given by $N_R$ terminated by the following two-terminal elements, as shown in Fig. 1:
- $\mathcal{D} \in \mathrm{C}_q$ in parallel to $\mathcal{D} \in \mathrm{M}_\varphi$ (we assume there are $n_{\gamma\mu}$ of such elements);
- $\mathcal{D} \in \mathrm{C}_q$ ($n_\gamma$);
- $\mathcal{D} \in \mathrm{L}_\varphi$ in in series with $\mathcal{D} \in \mathrm{M}_q$ ($n_{\lambda\mu}$);
- $\mathcal{D} \in \mathrm{L}_\varphi$ ($n_\lambda$).

Assume that there exists the hybrid representation of $N_R$
$$\begin{pmatrix} \mathbf{q}^{\gamma\mu}(t;t_0) \\ \boldsymbol{\varphi}^{\lambda\mu}(t;t_0) \\ \mathbf{q}^{\gamma}(t;t_0) \\ \boldsymbol{\varphi}^{\lambda}(t;t_0) \end{pmatrix} = \mathbf{H} \begin{pmatrix} \boldsymbol{\varphi}^{\gamma\mu}(t;t_0) \\ \mathbf{q}^{\lambda\mu}(t;t_0) \\ \boldsymbol{\varphi}^{\gamma}(t;t_0) \\ \mathbf{q}^{\lambda}(t;t_0) \end{pmatrix} + \mathbf{U}(t;t_0) \qquad (1)$$
where
$$\mathbf{U}(t;t_0) = \mathbf{B} \begin{pmatrix} \boldsymbol{\varphi}_e(t;t_0) \\ \mathbf{q}_a(t;t_0) \end{pmatrix}$$
depends upon the flux and charge sources within $N_R$.

*Remark 1:* A necessary condition for the existence of the hybrid representation (1) is that $N$ has no loop formed by

capacitors and independent flux sources only, and no cut-set formed by inductors and current sources only. Moreover, according to [19, Th. 2], for the existence of (1), each flux-controlled memristor should be in parallel to a capacitor, while each charge-controlled memristor should be in series with an inductor. Finally, according to the SE representations in (3.8) and (3.9) in [19], we need to exclude nonlinear capacitors that are not charge-controlled and nonlinear inductors that are not flux-controlled. This justifies the previous choices of elements in $N$ guaranteeing the existence of the SE representation.

For the $n_{\gamma\mu}$ two-terminal elements $\mathrm{C}_q$-$\mathrm{M}_\varphi$, in vector form, the CR can be written as

$$-\mathbf{q}^{\gamma\mu}(t;t_0)=\mathbf{f}_M^{\gamma\mu}(\boldsymbol{\varphi}^{\gamma\mu}(t;t_0)+\boldsymbol{\varphi}_{M0}^{\gamma\mu})-\mathbf{f}_M^{\gamma\mu}(\boldsymbol{\varphi}_{M0}^{\gamma\mu})+\mathbf{q}_C^{\gamma\mu}(t;t_0) \tag{2}$$

with

$$\dot{\boldsymbol{\varphi}}^{\gamma\mu}(t;t_0)=\mathbf{f}_C^{\gamma\mu}(\mathbf{q}_C^{\gamma\mu}(t;t_0)+\mathbf{q}_{C0}^{\gamma\mu}).$$

For the $n_\gamma$ two-terminal elements $\mathrm{C}_q$ we have

$$\dot{\boldsymbol{\varphi}}^{\gamma}(t;t_0)=\mathbf{f}_C^{\gamma}(\mathbf{q}_C^{\gamma}(t;t_0)+\mathbf{q}_{C0}^{\gamma}). \tag{3}$$

For the $n_{\lambda\mu}$ two-terminal elements $\mathrm{L}_\varphi$-$\mathrm{M}_q$ we obtain

$$-\boldsymbol{\varphi}^{\lambda\mu}(t;t_0)=\mathbf{f}_M^{\lambda\mu}(\mathbf{q}^{\lambda\mu}(t;t_0)+\mathbf{q}_{M0}^{\lambda\mu})-\mathbf{f}_M^{\lambda\mu}(\mathbf{q}_{M0}^{\lambda\mu})+\boldsymbol{\varphi}_L^{\lambda\mu}(t;t_0) \tag{4}$$

with

$$\dot{\mathbf{q}}^{\lambda\mu}(t;t_0)=\mathbf{f}_L^{\lambda\mu}(\boldsymbol{\varphi}_L^{\lambda\mu}(t;t_0)+\boldsymbol{\varphi}_{L0}^{\lambda\mu})$$

while for the $n_\lambda$ two-terminal elements $\mathrm{L}_\varphi$ we have

$$\dot{\mathbf{q}}^{\lambda}(t;t_0)=\mathbf{f}_L^{\lambda}(\boldsymbol{\varphi}_L^{\lambda}(t;t_0)+\boldsymbol{\varphi}_{L0}^{\lambda}). \tag{5}$$

Let us introduce the vectors of incremental capacitor fluxes and incremental inductor charges

$$\mathbf{x}(t)=\begin{pmatrix}\boldsymbol{\varphi}^{\gamma\mu}(t;t_0)\\ \mathbf{q}^{\lambda\mu}(t;t_0)\end{pmatrix}=\begin{pmatrix}\boldsymbol{\varphi}_C^{\gamma\mu}(t;t_0)\\ \mathbf{q}_L^{\lambda\mu}(t;t_0)\end{pmatrix}$$

$$\mathbf{y}(t)=\begin{pmatrix}\boldsymbol{\varphi}^{\gamma}(t;t_0)\\ \mathbf{q}^{\lambda}(t;t_0)\end{pmatrix}=\begin{pmatrix}\boldsymbol{\varphi}_C^{\gamma}(t;t_0)\\ \mathbf{q}_L^{\lambda}(t;t_0)\end{pmatrix}$$

and the auxiliary vectors

$$\mathbf{w}(t)=\begin{pmatrix}\mathbf{q}_C^{\gamma\mu}(t;t_0)\\ \boldsymbol{\varphi}_L^{\lambda\mu}(t;t_0)\end{pmatrix};\quad \mathbf{z}(t)=\begin{pmatrix}\mathbf{q}_C^{\gamma}(t;t_0)\\ \boldsymbol{\varphi}_L^{\lambda}(t;t_0)\end{pmatrix}.$$

Consider also the vectors of the memristor fluxes and charges and the capacitor charges and inductor fluxes

$$\mathbf{X}(t)=\mathbf{x}(t)+\mathbf{X}_0=\begin{pmatrix}\boldsymbol{\varphi}_M^{\gamma\mu}(t)\\ \mathbf{q}_M^{\lambda\mu}(t)\end{pmatrix} \tag{6}$$

$$\mathbf{W}(t)=\mathbf{w}(t)+\mathbf{W}_0=\begin{pmatrix}\mathbf{q}_C^{\gamma\mu}(t)\\ \boldsymbol{\varphi}_L^{\lambda\mu}(t)\end{pmatrix} \tag{7}$$

$$\mathbf{Z}(t)=\mathbf{z}(t)+\mathbf{Z}_0=\begin{pmatrix}\mathbf{q}_C^{\gamma}(t)\\ \boldsymbol{\varphi}_L^{\lambda}(t)\end{pmatrix} \tag{8}$$

where the vectors of initial conditions for the same variables are

$$\mathbf{X}_0=\begin{pmatrix}\boldsymbol{\varphi}_{M0}^{\gamma\mu}\\ \mathbf{q}_{M0}^{\lambda\mu}\end{pmatrix};\quad \mathbf{W}_0=\begin{pmatrix}\mathbf{q}_{C0}^{\gamma\mu}\\ \boldsymbol{\varphi}_{L0}^{\lambda\mu}\end{pmatrix};\quad \mathbf{Z}_0=\begin{pmatrix}\mathbf{q}_{C0}^{\gamma}\\ \boldsymbol{\varphi}_{L0}^{\lambda}\end{pmatrix}.$$

Finally, define the following nonlinear functions

$$\mathbf{F}^a(\cdot)=\begin{pmatrix}\mathbf{f}_M^{\gamma\mu}(\cdot)\\ \mathbf{f}_M^{\lambda\mu}(\cdot)\end{pmatrix};\quad \mathbf{F}^b(\cdot)=\begin{pmatrix}\mathbf{f}_C^{\gamma\mu}(\cdot)\\ \mathbf{f}_L^{\lambda\mu}(\cdot)\end{pmatrix};\quad \mathbf{F}^c(\cdot)=\begin{pmatrix}\mathbf{f}_C^{\gamma}(\cdot)\\ \mathbf{f}_L^{\lambda}(\cdot)\end{pmatrix}$$

and decompose matrices $\mathbf{H}=\{\mathbf{H}_{ij}\}$, $\mathbf{B}=\{\mathbf{B}_{ij}\}$, $i,j=1,2$, and vector $\mathbf{U}(t;t_0)=\{\mathbf{U}_i(t;t_0)\}$, $i=1,2$.

Substituting (2)-(5) in (1) we obtain that the SEs of $N$ in the $(\varphi,q)$-domain can be expressed as [18]

$$\begin{pmatrix}\dot{\mathbf{x}}(t)\\ \dot{\mathbf{y}}(t)\end{pmatrix}=\begin{pmatrix}\mathbf{F}^b(\mathbf{w}(t)+\mathbf{W}_0)\\ \mathbf{F}^c(\mathbf{z}(t)+\mathbf{Z}_0)\end{pmatrix}$$

where

$$\begin{pmatrix}\mathbf{w}(t)\\ \mathbf{z}(t)\end{pmatrix}=\begin{pmatrix}-\mathbf{F}^a(\mathbf{x}(t)+\mathbf{X}_0)+\mathbf{F}^a(\mathbf{X}_0)\\ \mathbf{0}\end{pmatrix}-\mathbf{H}\begin{pmatrix}\mathbf{x}(t)\\ \mathbf{y}(t)\end{pmatrix}-\mathbf{U}(t;t_0). \tag{9}$$

In a more compact form the same SEs can be written as

$$\dot{\mathbf{x}}(t)=\mathbf{F}^b\big(-\mathbf{F}^a(\mathbf{x}(t)+\mathbf{X}_0)+\mathbf{F}^a(\mathbf{X}_0)-\mathbf{H}_{11}\mathbf{x}(t)-\mathbf{H}_{12}\mathbf{y}(t)-\mathbf{U}_1(t;t_0)+\mathbf{W}_0\big) \tag{10}$$

$$\dot{\mathbf{y}}(t)=\mathbf{F}^c(-\mathbf{H}_{21}\mathbf{x}(t)-\mathbf{H}_{22}\mathbf{y}(t)-\mathbf{U}_2(t;t_0)+\mathbf{Z}_0) \tag{11}$$

for $t\geq t_0$, with initial condition $(\mathbf{x}(t_0),\mathbf{y}(t_0))=(\mathbf{0},\mathbf{0})$.

This is a system of $n_{\varphi q}=n_{\gamma\mu}+n_{\lambda\mu}+n_\gamma+n_\lambda$ equations in the same number of state variables $(\mathbf{x}(t),\mathbf{y}(t))\in\mathbb{R}^{n_{\varphi q}}$ given by the incremental capacitor fluxes and incremental inductor charges. The order of the SEs in the $(\varphi,q)$-domain is $n_{\varphi q}$.

### *B. State Equations in the $(v,i)$-Domain*

The SEs of $N$ in the $(v,i)$-domain can be obtained by differentiation in time of (1)-(5) and by performing substitutions analogous to those used to derive SEs (9). We obtain

$$\dot{\mathbf{X}}(t)=\mathbf{F}^b(\mathbf{W}(t)) \tag{12}$$

$$\begin{pmatrix}\dot{\mathbf{W}}(t)\\ \dot{\mathbf{Z}}(t)\end{pmatrix}=\begin{pmatrix}-\mathbf{J}_{\mathbf{F}^a}(\mathbf{X}(t))\mathbf{F}^b(\mathbf{W}(t))\\ \mathbf{0}\end{pmatrix}-\mathbf{H}\begin{pmatrix}\mathbf{F}^b(\mathbf{W}(t))\\ \mathbf{F}^c(\mathbf{Z}(t))\end{pmatrix}-\dot{\mathbf{U}}(t;t_0) \tag{13}$$

for $t\geq t_0$, with initial condition

$$\boldsymbol{\Gamma}_0=(\mathbf{X}(t_0),\mathbf{W}(t_0),\mathbf{Z}(t_0))=(\mathbf{X}_0,\mathbf{W}_0,\mathbf{Z}_0)$$

where $\mathbf{J}_{\mathbf{F}^a}$ denotes the Jacobian of $\mathbf{F}^a$.

This is a system of $n_{vi}=2(n_{\gamma\mu}+n_{\lambda\mu})+n_\gamma+n_\lambda$ equations in the same number of state variables

$$\boldsymbol{\Gamma}(t)=(\mathbf{X}(t),\mathbf{W}(t),\mathbf{Z}(t))\in\mathbb{R}^{n_{vi}}$$

given by the fluxes of flux-controlled memristors, charges of charge-controlled memristors, charges of capacitors and fluxes of inductors. The order of the SEs in the $(v,i)$-domain is $n_{vi}$.

*Remark 2:* Note that for the SE description there is a reduction of order $n_{\gamma\mu}+n_{\lambda\mu}$, equal to the number of memristors, passing from the $(v,i)$-domain to the $(\varphi,q)$-domain.

## III. Invariant Manifolds and Coexisting Dynamics

Let us now address the main issues concerning the existence of invariant manifolds and coexisting reduced-order dynamics and attractors.

Consider, under the assumption $\det \mathbf{H}_{22} \neq 0$, function $\mathbf{K}(\mathbf{\Gamma}) : \mathbb{R}^{n_{vi}} \rightarrow \mathbb{R}^{n_{\gamma\mu}+n_{\lambda\mu}}$ of the state variables in the $(v, i)$-domain defined as

$$\mathbf{K}(\mathbf{\Gamma}) = \mathbf{F}^a(\mathbf{X}) + \mathbf{S}_{22}\mathbf{X} + \mathbf{W} - \mathbf{H}_{12}\mathbf{H}_{22}^{-1}\mathbf{Z} \tag{14}$$

where $\mathbf{S}_{22} = \mathbf{H}_{11} - \mathbf{H}_{12}\mathbf{H}_{22}^{-1}\mathbf{H}_{21}$.

Let $\Omega = \mathbf{K}(\mathbb{R}^{n_{vi}})$. For any $\bar{\mathbf{\Gamma}} \in \Omega$, consider the set

$$\mathcal{M}(\bar{\mathbf{\Gamma}}) = \{\mathbf{\Gamma} \in \mathbb{R}^{n_{vi}} : \mathbf{K}(\mathbf{\Gamma}) = \bar{\mathbf{\Gamma}}\}.$$

This defines $\infty^{n_{\gamma\mu}+n_{\lambda\mu}}$ manifolds in the state space $\mathbb{R}^{n_{vi}}$ in the $(v, i)$-domain with geometric properties analogous to those in Theorem 1 in [16].

*Theorem 1:* Assume $\det \mathbf{H}_{22} \neq 0$ and let $\mathbf{\Gamma}(t; t_0, \mathbf{\Gamma}_0)$, $t \geq t_0$, where $\mathbf{\Gamma}_0 \in \mathbb{R}^{n_{vi}}$, be the solution of the SEs in the $(v, i)$-domain with initial condition $\mathbf{\Gamma}_0$ at $t_0$. Then, for any $t \geq t_0$ we have

$$\mathbf{\Gamma}(t; t_0, \mathbf{\Gamma}_0) \in \mathcal{M}(\mathbf{K}(\mathbf{\Gamma}(t; t_0, \mathbf{\Gamma}_0)))$$

where

$$\begin{aligned}\mathbf{K}(\mathbf{\Gamma}(t; t_0, \mathbf{\Gamma}_0)) = \mathbf{K}(\mathbf{\Gamma_0}) &+ \mathbf{H}_{12}\mathbf{H}_{22}^{-1}(\mathbf{B}_{21}\boldsymbol{\varphi}_e(t; t_0) \\ &+ \mathbf{B}_{22}\mathbf{q}_a(t; t_0)) \\ &- (\mathbf{B}_{11}\boldsymbol{\varphi}_e(t; t_0) + \mathbf{B}_{12}\mathbf{q}_a(t; t_0)).\end{aligned} \tag{15}$$

*Proof:* From (9) we obtain $\mathbf{z}(t) = -\mathbf{H}_{21}\mathbf{x}(t) - \mathbf{H}_{22}\mathbf{y}(t) - \mathbf{U}_2(t; t_0)$ and, since $\det \mathbf{H}_{22} \neq 0$

$$\mathbf{y}(t) = -\mathbf{H}_{22}^{-1}(\mathbf{z}(t) + \mathbf{H}_{21}\mathbf{x}(t) + \mathbf{U}_2(t; t_0)).$$

Substituting in (9)

$$\begin{aligned}\mathbf{0} = \mathbf{F}^a(\mathbf{x}(t) + \mathbf{X}_0) - \mathbf{F}^a(\mathbf{X}_0) + \mathbf{S}_{22}\mathbf{x}(t) + \mathbf{w}(t) \\ - \mathbf{H}_{12}\mathbf{H}_{22}^{-1}\mathbf{z}(t) - \mathbf{H}_{12}\mathbf{H}_{22}^{-1}\mathbf{U}_2(t; t_0) + \mathbf{U}_1(t; t_0)\end{aligned}$$

for any $t \geq t_0$, where $\mathbf{S}_{22} = \mathbf{H}_{11} - \mathbf{H}_{12}\mathbf{H}_{22}^{-1}\mathbf{H}_{21}$. Then, the result in the theorem follows. ■

Let us now study the behavior of $N$ in the inputless case. The following holds.

*Theorem 2:* Assume $\det \mathbf{H}_{22} \neq 0$. Consider the inputless case $\boldsymbol{\varphi}_e(t; t_0) = 0$, $\mathbf{q}_a(t; t_0) = 0$, for any $t \geq t_0$. Then:

1) each manifold $\mathcal{M}$ is positively invariant for the dynamics of $N$ in the $(v, i)$-domain, namely, given any initial condition $\mathbf{\Gamma}_0$, we have

$$\mathbf{\Gamma}(t; t_0, \mathbf{\Gamma}_0) \in \mathcal{M}(\mathbf{K}(\mathbf{\Gamma}_0))$$

for any $t \geq t_0$;

2) the reduced-order ($n_{\varphi q}$-order) system on manifold $\mathcal{M}(\mathbf{K}(\mathbf{\Gamma}_0))$ is given by

$$\begin{aligned}\dot{\mathbf{X}}(t) = \mathbf{F}^b\big(&- \mathbf{F}^a(\mathbf{X}(t)) - \mathbf{H}_{11}\mathbf{X}(t) - \mathbf{H}_{12}\mathbf{Y}(t) \\ &+ \mathbf{K}(\mathbf{\Gamma}_0)\big)\end{aligned} \tag{16}$$

$$\dot{\mathbf{Y}}(t) = \mathbf{F}^c(-\mathbf{H}_{21}\mathbf{X}(t) - \mathbf{H}_{22}\mathbf{Y}(t)) \tag{17}$$

where

$$\mathbf{Y}(t) = \mathbf{y}(t) - \mathbf{H}_{22}^{-1}(\mathbf{H}_{21}\mathbf{X}_0 + \mathbf{Z}_0). \tag{18}$$

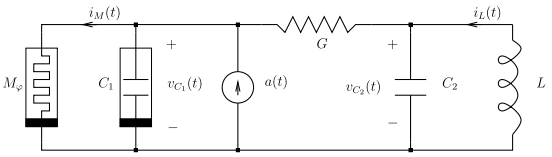


Fig. 2. Modified Chua's circuit with memristor and nonlinear capacitor.

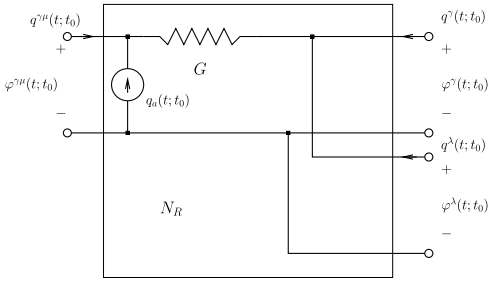


Fig. 3. Three-port $N_R$ for finding the hybrid representation of the modified Chua's circuit.

*Proof:* In the inputless case, it follows from (15) of Theorem 1 that $\mathbf{K}(\mathbf{\Gamma}(t; t_0, \mathbf{\Gamma}_0)) = \mathbf{K}(\mathbf{\Gamma}_0)$ for any $t \geq t_0$, as stated in point 1).

To prove point 2), it is enough to substitute (18) in (10), (11), note that $\dot{\mathbf{y}}(\cdot) = \dot{\mathbf{Y}}(\cdot)$ and recall (6)-(8). ■

Consider the constant term $\mathbf{K}_0 = \mathbf{K}(\mathbf{\Gamma}_0)$ at the right-hand side of the reduced-order system (16). If we change the initial conditions $\mathbf{\Gamma}_0$ in a way that also $\mathbf{K}(\mathbf{\Gamma}_0)$ is changed, then we obtain a different reduced order dynamics on manifold $\mathcal{M}(\mathbf{K}_0)$. This explains theoretically why for structural reasons there coexist infinitely many different reduced-order dynamics and attractors for a given circuit $N \in \mathcal{N}$.

Let us now consider the case where the inputs are non-zero. On the basis of (15), we can design independent pulse voltage or current source to steer the solutions of $N$ through different manifolds and dynamics along the lines discussed in [16]. This latter aspect is further illustrated via the examples in the next sections.

## IV. Chua's Circuit With Memristor and Nonlinear Capacitor

To illustrate the unfolding of the dynamics of circuits with memristors and nonlinear storage elements, we consider a variant of Chua's circuit where the nonlinear resistor (Chua's diode) is replaced by a flux-controlled memristor $M_\varphi$ with characteristic $q_M = f_M(\varphi_M)$ and one linear capacitor is replaced by a nonlinear charge-controlled capacitor $C_1$ with characteristic $v_{C_1} = f_{C_1}(q_{C_1})$ (Fig. 2). An independent current source $a(\cdot)$ is also introduced for manifold programming.

To obtain the hybrid representation of the three-port $N_R$ for this circuit, let us refer to Fig. 3. A simple analysis yields

$$\begin{pmatrix} q^{\gamma\mu}(t; t_0) \\ q^{\gamma}(t; t_0) \\ \varphi^{\lambda}(t; t_0) \end{pmatrix} = \mathbf{H} \begin{pmatrix} \varphi^{\gamma\mu}(t; t_0) \\ \varphi^{\gamma}(t; t_0) \\ q^{\lambda}(t; t_0) \end{pmatrix} + \mathbf{B}q_a(t; t_0)$$

with

$$\mathbf{H} = \begin{pmatrix} G & -G & 0 \\ -G & G & -1 \\ 0 & 1 & 0 \end{pmatrix}, \quad \mathbf{B} = \begin{pmatrix} -1 \\ 0 \\ 0 \end{pmatrix}$$

and $q_a(t; t_0) = \int_{t_0}^{t} a(\tau)d\tau$.

We have $x(t) = \varphi_{C_1}(t; t_0)$, $\mathbf{y}(t) = (\varphi_{C_2}(t; t_0), q_L(t; t_0))^T$ and $w(t) = q_{C_1}(t; t_0)$, $\mathbf{z}(t) = (q_{C_2}(t; t_0), \varphi_L(t; t_0))^T$, where $T$ denotes the transpose. Then, on the basis of (10), (11) we obtain that the modified Chua's circuit satisfies the following third-order system of SEs in the $(\varphi, q)$-domain

$$\begin{aligned}\dot{\varphi}_{C_1}(t; t_0) = f_{C_1}\big( &- G\varphi_{C_1}(t; t_0) + G\varphi_{C_2}(t; t_0) \\ &- f_M(\varphi_{C_1}(t; t_0) + \varphi_{M_0}) + f_M(\varphi_{M_0}) \\ &+ q_{C_{10}} + q_a(t; t_0)\big) \qquad (19)\\ \dot{\varphi}_{C_2}(t; t_0) = \frac{1}{C_2}[&G\varphi_{C_1}(t; t_0) - G\varphi_{C_2}(t; t_0) \\ &+ q_L(t; t_0) + q_{C_{20}}] \qquad (20)\\ \dot{q}_L(t; t_0) = \frac{1}{L}[&-q_{C_2}(t; t_0) - q_{L_0}]. \qquad (21)\end{aligned}$$

The initial conditions are $\varphi_{C_1}(t_0; t_0) = \varphi_{C_2}(t_0; t_0) = 0$ and $q_L(t_0, t_0) = 0$.

By means of (12), (13) we obtain the fourth-order SEs in the $(\upsilon, i)$-domain

$$\begin{aligned}\dot{\varphi}_M(t) &= f_{C_1}(q_{C_1}(t))\\ \dot{q}_{C_1}(t) &= G\left[\frac{q_{C_2}(t)}{C_2} - f_{C_1}(q_{C_1}(t))\right]\\ &\quad - f'_M(\varphi_M(t))\, f_{C_1}(q_{C_1}(t)) + a(t)\\ \dot{q}_{C_2}(t) &= \frac{\varphi_L(t)}{L} + G f_{C_1}(q_{C_1}(t)) - \frac{G q_{C_2}(t)}{C_2}\\ \frac{d\varphi_L(t)}{dt} &= -\frac{q_{C_2}(t)}{C_2}\end{aligned}$$

with initial conditions $\varphi_{M_0}$, $q_{C_{10}}$, $q_{C_{20}}$ and $\varphi_{L_0}$.

We have

$$\det \mathbf{H}_{22} = \det \begin{pmatrix} G & -1 \\ 1 & 0 \end{pmatrix} = 1 \neq 0.$$

Let $\mathbf{\Gamma}(t) = (\varphi_M(t), q_{C_1}(t), q_{C_2}(t), \varphi_L(t))^T \in \mathbb{R}^4$ be the vector of state variables in the $(\upsilon, i)$-domain. A simple computation yields $S_{22} = G$ and $\mathbf{H}_{12}\mathbf{H}_{22}^{-1} = [0\ G]$. Then, from (14) we obtain

$$\begin{aligned}K(\mathbf{\Gamma}(t)) \doteq Q(t) = f_M(\varphi_M(t)) + G\varphi_M(t)&\\ + q_{C_1}(t) + G\varphi_L(t) : \mathbb{R}^4 \to \mathbb{R}&\end{aligned}$$

for any $t \geq t_0$. The state-space $\mathbb{R}^4$ in the $(\upsilon, i)$-domain can be decomposed in $\infty^1$ manifolds

$$\begin{aligned}\mathcal{M}(Q_0) = \{(\varphi_M, q_{C_1}, q_{C_2}, \varphi_L)^T : f_M(\varphi_M(t)) + G\varphi_M(t) \qquad (22)\\ + q_{C_1}(t) + G\varphi_L(t) = Q_0\} \qquad (23)\end{aligned}$$

for any $Q_0 \in \mathbb{R}$. Moreover, from (15) we have

$$Q(t) = Q_0 + q_a(t; t_0) \qquad (24)$$

for any $t \geq t_0$, where $Q_0 = Q(t_0)$.

Consider first the inputless case $a(t) = 0$, hence $q_a(t; t_0) = 0$, for any $t \geq t_0$. Due to Theorem 2, manifolds $\mathcal{M}(\cdot)$ are positively invariant for the dynamics in the $(\upsilon, i)$-domain. Namely, given the initial conditions $\mathbf{\Gamma}_0 = (\varphi_{M_0}, q_{C_{10}}, q_{C_{20}}, \varphi_{L_0})^T$, if we let $Q_0 = K(\mathbf{\Gamma}_0)$, then we have $\mathbf{\Gamma}(t; t_0, \mathbf{\Gamma}_0) \in \mathcal{M}(Q_0)$ for any $t \geq t_0$. Moreover,

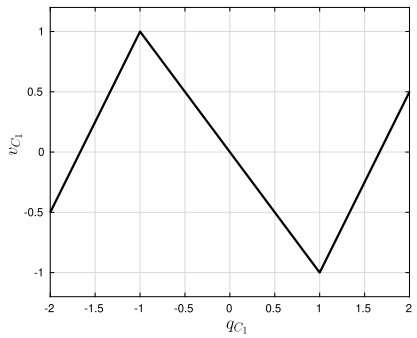


Fig. 4. Nonlinear characteristic $f_{C_1}$ of $C_1$.

from (16) and (17), the reduced-order (third-order) system describing the dynamics on $\mathcal{M}(Q_0)$ is given by

$$\begin{aligned}\dot{X}(t) &= f_{C_1}\big(-GX(t) + GY_1(t) - f_M(X(t)) + Q_0\big)\\ \dot{Y}_1(t) &= \frac{1}{C_2}[GX(t) - GY_1(t) + Y_2(t)]\\ \dot{Y}_2(t) &= \frac{1}{L}(-Y_1(t)) \qquad (25)\end{aligned}$$

where $\varphi_M(t) = X(t)$ and

$$\begin{pmatrix} Y_1(t) \\ Y_2(t) \end{pmatrix} = \begin{pmatrix} \varphi_{C_2}(t) - \varphi_{L_0} - \varphi_{C_{20}} \\ q_L(t) - q_{L_0} - G\varphi_{M_0} + q_{C_{20}} - G\varphi_{L_0} \end{pmatrix}.$$

Summing up, each invariant manifold $\mathcal{M}(Q_0)$ is identified by quantity $Q_0 = K(\mathbf{\Gamma}_0) = f_M(\varphi_{M_0}) + G\varphi_{M_0} + q_{C_{10}} + G\varphi_{L_0}$ (cf. (22)). Moreover, the same value of $Q_0$ acts as an additional parameter, i.e., a forcing term, for the vector field defining the reduced-order system on $\mathcal{M}(Q_0)$ (cf. (25)). Different manifolds are characterized by different values of $Q_0$ and, hence, different dynamics. This proves analytically that there is *coexistence* of infinitely many different third-order dynamics for a *fixed* set of circuit parameters. Also, note that it is possible to vary $Q_0$ in $\mathbb{R}$ by *varying the initial conditions* $\mathbf{\Gamma}_0 = (\varphi_{M_0}, q_{C_{10}}, q_{C_{20}}, \varphi_{L_0})^T$ for the state variables in the $(\upsilon, i)$-domain, for fixed circuit parameters. Then, we expect to observe bifurcations due to varying the initial conditions, for a fixed set of circuit parameters. This kind of bifurcations is named bifurcations without parameters [14]. Some of these phenomena are illustrated via the next numerical simulations.

Suppose that the nonlinear characteristic of $C_1$ is the piecewise linear function

$$\begin{aligned}\upsilon_{C_1} &= f_{C_1}(q_{C_1}) \qquad (26)\\ &= \frac{1}{C_b} q_{C_1} + \frac{1}{2}\left(\frac{1}{C_b} - \frac{1}{C_a}\right)(|q_{C_1} - q_0| - |q_{C_1} + q_0|) \qquad (27)\end{aligned}$$

with $1/C_a = -1$, $1/C_b = 1.5$ and $q_0 = 1$ (Fig. 4), while the memristor characteristic is

$$q_M = f_M(\varphi_M) = \alpha\varphi_M + \frac{1}{3}\beta\varphi_M^3 \qquad (28)$$

with $\alpha = -1/2$ and $\beta = 0.015$. Note that the memristor is active since its memristance is negative in an interval around the value $\varphi_M = 0$. Moreover, let $G = 1$, $C_2 = 8.8$ and $L = C_2/14$.

Figure 5 reports the bifurcation diagram of the SEs in the $(\varphi, q)$-domain (19)-(21), obtained by increasing $Q_0$ in

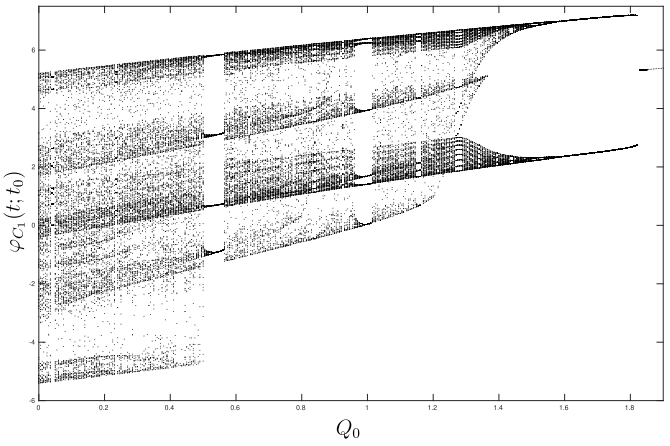


Fig. 5. Bifurcation diagram of the modified Chua's circuit obtained by varying $Q_0$ for a fixed set of circuit parameters, namely, $f_{C_1}$ as in (26), $f_M$ as in (28) and $G = 1$, $C_2 = 8.8$, $L = C_2/14$.

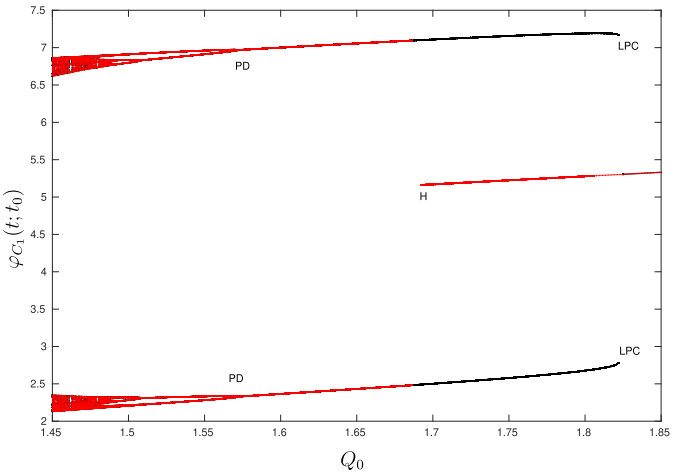


Fig. 6. Magnification of the bifurcation diagram of Fig. 5. Black dots are obtained by increasing $Q_0$ in the interval $[1.45, 1.85]$, while red dots are obtained by decreasing $Q_0$. A sequence of period-doubling (PD) bifurcations can be detected. Moreover, a scenario is suggested where there is a subcritical Hopf bifurcation (H) and a saddle-node bifurcation of periodic orbits (LPC–limit point of cycles).

small steps $\Delta Q_0 = 0.005$, for fixed circuit parameters. Note that there are intervals where the circuit displays complex dynamics, intervals with a periodic dynamics (cycles with period 3, 2 and 1) and an interval with a convergent dynamics. Figure 6 provides a magnified version of the bifurcation diagram for $Q_0 \in [1.45, 1.85]$, where we can better detect a sequence of inverse period-doubling (PD) bifurcations destroying the complex attractor and leading to a periodic dynamics (cycle with period 1). The last PD is at $Q_0 = 1.573$. The same figure reports with red dots a simulation obtained by decreasing $Q_0$. The figure suggests a scenario with a subcritical Hopf (H) bifurcation for $Q_0 = 1.695$ and a saddle-node bifurcation of periodic orbits (LPC–limit point of cycles) at $Q_0 = 1.822$. Note that there is coexistence of a stable cycle and a stable equilibrium point when $Q_0 \in [1.695, 1.822]$. Since such figures are obtained by varying $Q_0$ via a variation of the initial conditions, for a fixed set

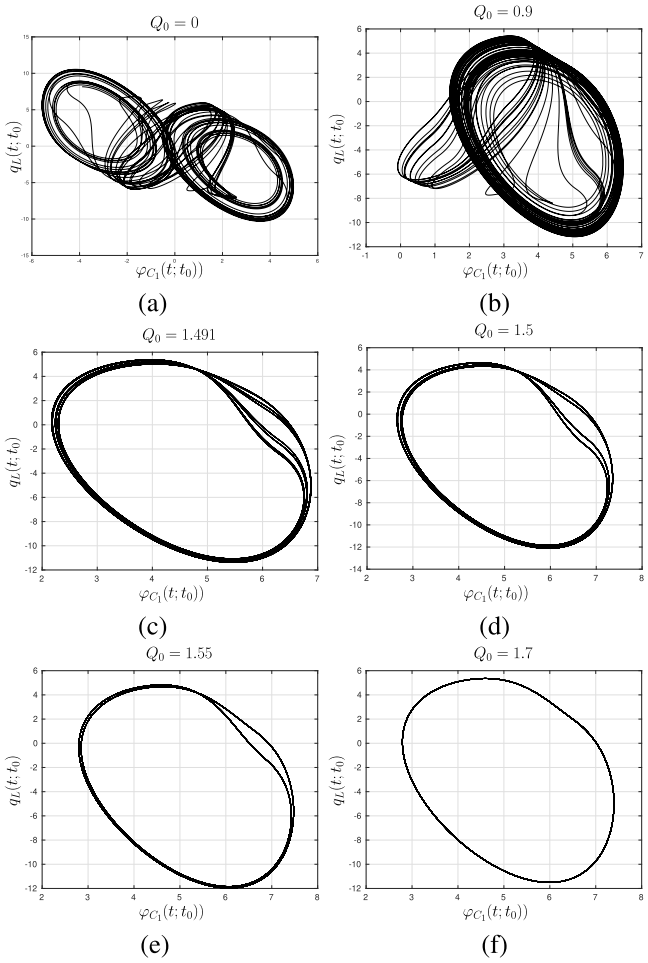


Fig. 7. Coexisting attractors displayed by the modified Chua's circuit obtained for different values of $Q_0$ and fixed circuit parameters: (a) double-scroll attractor ($Q_0 = 0$); single-scroll attractor ($Q_0 = 0.9$); cycle with period eight ($Q_0 = 1.491$); cycle with period four ($Q_0 = 1.5$); cycle with period 2 ($Q_0 = 1.55$) and cycle with period 1 ($Q_0 = 1.7$).

of circuit parameters, the numerical simulations confirm the theoretic findings, i.e., there is coexistence of different chaotic attractors, cycles with different periods and also convergent dynamics for the memristor circuit. Moreover, several types of bifurcations without parameters are observed.

Figure 7 reports the shapes of the different attractors for better illustrating the dynamics complexity. Figure 7(a) depicts the attractor when the initial conditions are such that $Q_0 = K(\mathbf{\Gamma}_0) = 0$, i.e., the dynamics evolve on the manifold $\mathcal{M}(0)$. It is seen that the solution (projection onto the $\varphi_{C_1} - q_L$ plane) has a complex attractor resembling the double-scroll attractor of Chua's circuit. The plots (b), (c), (d), (e), and (f) in the same figure then show the simulations when the initial conditions are respectively chosen in a way that $Q_0 = \{0.9, 1.491, 1.5, 1.55, 1.7\}$.

In a second experiment we use the input $a(t)$ to steer trajectories of the modified Chua's circuit through different manifolds and attractors. Suppose that at $t_0 = 0$ the circuit in on manifold $\mathcal{M}(Q_0 = 0)$, i.e., $\mathbf{\Gamma}_0 \in \mathcal{M}(0)$ and let $\mathbf{\Gamma}(t; 0, \mathbf{\Gamma}_0)$ be the corresponding solution of the circuit. Let $a(\cdot)$ be given by a sequence of three short rectangular pulses

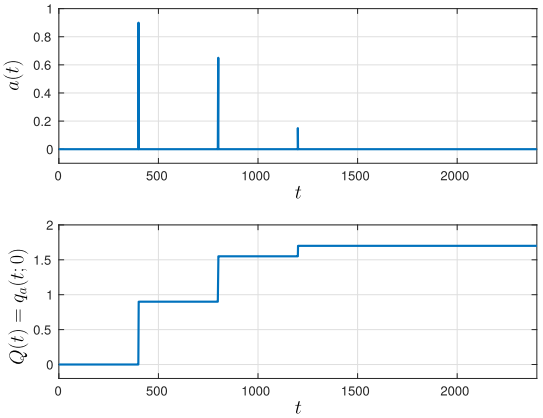


Fig. 8. Input signal $a(\cdot)$ given by a sequence of three short rectangular impulses (upper plot) and time-domain behavior of $Q(t) = q_a(t;0) = \int_0^t a(\tau)d\tau$ (lower plot).

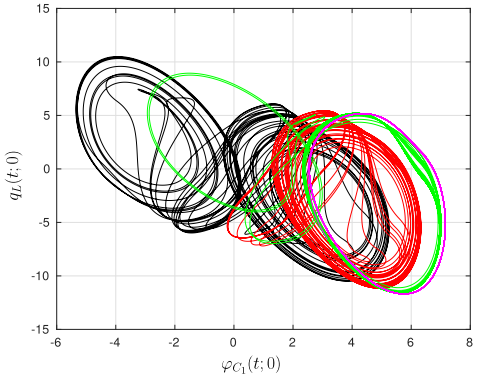


Fig. 9. Projection onto the $\varphi_{C1} - q_L$ plane of a trajectory of a modified Chua's circuit that is driven through different manifolds via the application of a pulse current source.

applied at $t_1 = 600$, $t_2 = 1200$ and $t_3 = 1800$ and suppose the length of each impulse is $\Delta = 1$ (normalized time), see Fig. 8. The first impulse has an area 0.9, the second has area 0.65 and the third one has area 0.15. The circuit evolves on $\mathcal{M}(0)$, and tends to a double-scroll chaotic attractor in $\mathcal{M}(0)$ up to the application of the first impulse. Consider now the first impulse. At $t_1 + \Delta$, when the impulse is over, we have from (24) that $Q(t_1 + \Delta) = Q_0 + \int_{t_1}^{t_1+\Delta} a(\tau)d\tau = 0.9$ (Fig. 8). Due to Theorem 1, $\mathbf{\Gamma}(t_1+\Delta) \in \mathcal{M}(K(\mathbf{\Gamma}(t_1+\Delta))) = \mathcal{M}(Q(t_1 + \Delta)) = \mathcal{M}(0.9)$. Then, the first input causes the solution to pass from manifold $\mathcal{M}(0)$ to $\mathcal{M}(0.9)$ in $[t_1, t_1+\Delta]$. In the interval $(t_1+\Delta, t_2)$ we have $a(t) = 0$, hence the solution stays on manifold $\mathcal{M}(0.9)$, where the solution displays a different (single-scroll) chaotic attractor. The second impulse has an analogous effect and causes the switch from $\mathcal{M}(0.9)$ to $\mathcal{M}(1.55)$, where the circuit tends to a period-two cycle. Finally, the third pulses drives the solution from $\mathcal{M}(1.55)$ to $\mathcal{M}(1.7)$ where the circuit has a period-one cycle. The corresponding simulation of the circuit in the $(\varphi, q)$-domain, shown in Fig. 9, confirms these theoretic results. For a better comparison, in Fig. 10 we also reported the superposition of the 4 attractors for manifolds $\mathcal{M}(0)$, $\mathcal{M}(0.9)$, $\mathcal{M}(1.55)$ and $\mathcal{M}(1.7)$ (cf. Fig. 7). We conclude that, using the pulse current

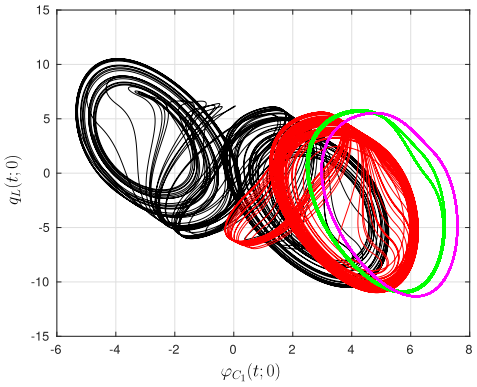


Fig. 10. Superposition of attractors of four different manifolds.

source $a(\cdot)$, we can easily and effectively drive solutions of the modified Chua's circuit through different manifolds, dynamics and attractors, without the need to alter the circuit parameters.

*Remark 3:* We have seen that an independent charge source $q_a(t; t_0)$ in parallel to $C_1$ permits to switch the modified Chua's circuit dynamics between different manifolds. It can be checked that an independent flux-source in series with $C_1$ would be instead ineffective to switch between different manifolds (details are omitted). An interesting issue for future investigation is to understand from a circuit topological viewpoint where to insert independent sources that make it possible the programming of different memristor dynamics.

*Remark 4:* Complex nonlinear dynamics are hard to simulate. We refer the reader to [21], [22] for a review and a discussion on the fidelity of numerical methods in such a context. Due to these issues, and in order that the interested readers can verify in detail the coexisting complex dynamics and bifurcations in the modified Chua's circuit, the code used in the numerical simulations of the paper is made available in platform Code Ocean.

*Remark 5:* Several papers in the literature reports on different dynamics and attractors that are observed by varying the initial conditions for a fixed set of memristor circuit parameters, see, e.g., [23], [24], and references therein. Unlike those papers, which are based on simulations or experiments, here we have proved analytically that for structural reasons there is coexistence of different dynamics and attractors in a memristor circuit. This phenomenon is due to the foliation property of the state space and the parameter $Q_0$, which depends upon the initial conditions, in the right-hand side of the vector field describing the dynamics on each manifold of the modified Chua's circuit.

## V. Relaxation Oscillator With Memristor and Nonlinear Inductor

As a second example, we consider in this section a relaxation oscillator implemented via the parallel connection of a memristor and a nonlinear inductor as shown in Fig. 11(a). The memristor is flux-controlled and has a CR $q_M = f_M(\varphi_M) = a\varphi_M + \frac{1}{3}\beta\varphi_M^3$, where $a < 0$ and $\beta > 0$ (Fig. 12(a)). The inductor has a CR $i_L = f_L(\varphi_L)$, where $f_L(\cdot)$ is a strictly monotone increasing function mapping $\mathbb{R}$ onto $\mathbb{R}$ as

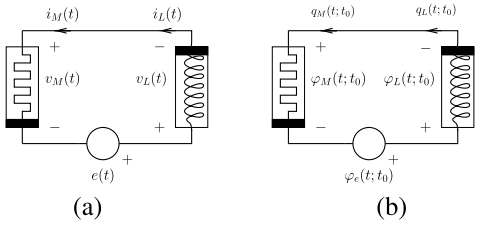


Fig. 11. (a) Relaxation oscillator with memristor and nonlinear inductor and (b) circuit in the $(\varphi, q)$-domain.

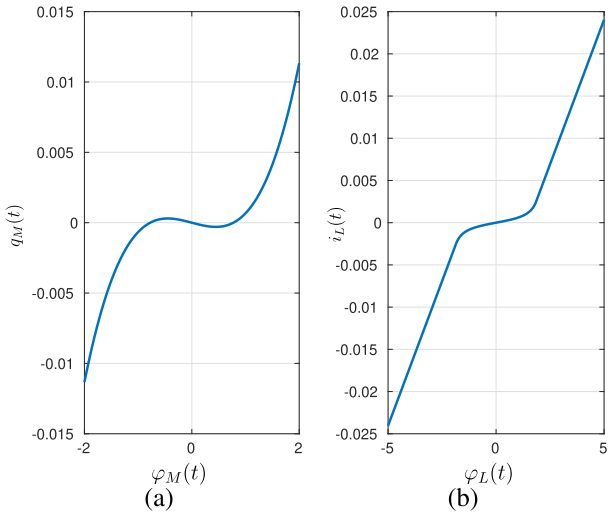


Fig. 12. (a) Nonlinear characteristic of the memristor and (b) of the nonlinear inductor.

in Fig. 12(b), hence it is is both flux- and current-controlled. A voltage source $e(\cdot)$ is also introduced for invariant-manifold programming purposes.

The circuit is obtained by the relaxation oscillator with tunnel diodes discussed in [25, Sect. IV] once the nonlinear resistor with two batteries and two tunnel diodes in push- pull configuration in Fig. 7 of that paper is replaced by a memristor with an analogous relationship between flux and charge.

The differential algebraic equations (DAEs) describing the circuit in the $(\varphi, q)$-domain are easily written as follows

$$\begin{aligned} q_L(t;t_0) &= q_M(t;t_0) \\ \varphi_M(t;t_0) &= -\varphi_L(t;t_0) + \varphi_e(t;t_0) \\ q_M(t;t_0) &= f_M(\varphi_M(t;t_0) + \varphi_{M0}) - f_M(\varphi_{M0}) \\ \dot{q}_L(t;t_0) &= f_L(\varphi_L(t;t_0) + \varphi_{L0}) \end{aligned}$$

where $\varphi_e(t;t_0) = \int_{t_0}^{t} e(\tau)d\tau$. These yield

$$\dot{q}_L(t;t_0) = f_L(\varphi_L(t;t_0) + \varphi_{L0}) \tag{29}$$

$$\begin{aligned} q_L(t;t_0) = {} & f_M(-\varphi_L(t;t_0) + \varphi_e(t;t_0) + \varphi_{M0}) \\ & - f_M(\varphi_{M0}). \end{aligned} \tag{30}$$

The dynamic route for the DAEs (29), (30) is depicted in Fig. 13 in the case where $\varphi_{L0} = 0, \varphi_{M0} = 0$ and $\varphi_e(t;t_0) = 0$. We are facing a classic situation where there are two forward impasse points $P_A$ and $P_B$ [19]. In fact, if the initial condition is such that $i_L(t_0) = i_{L0} > 0$, then the corresponding solution reaches $P_A$ in finite time and it cannot be further prolonged

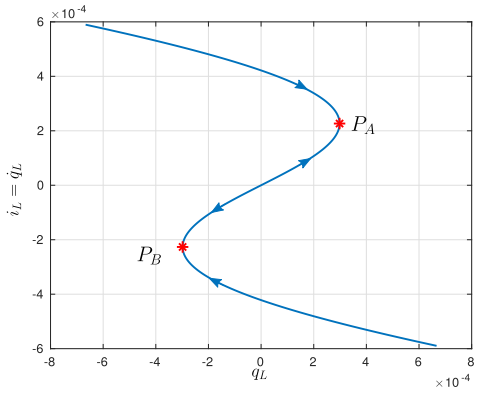


Fig. 13. Dynamic route with two impasse points $P_A$ and $P_B$.

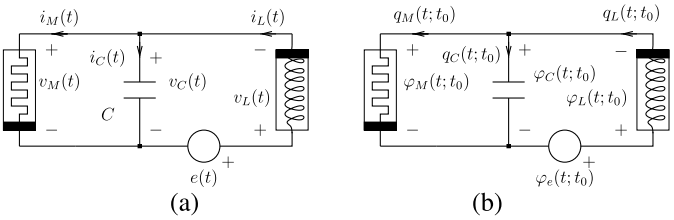


Fig. 14. (a) Circuit with a parasitic capacitance $C$ for breaking impasse points and (b) circuit in the $(\varphi, q)$-domain.

in time. Note that $P_A$ is not an equilibrium point, since $\dot{q}_L \neq 0$ at $P_A$, so we reached an absurd. An analogous situation is observed if $i_{L0} < 0$. It is not possible to write a local SE in a neighborhood of points $P_A$ and $P_B$, hence a global SE representation does not exist for the circuit. Solutions are defined up to a finite instant but cannot be prolonger thereafter, hence, the circuit is bad-modeled from a physical viewpoint. This situation is different from that studied in Section II, where a global SE is instead guaranteed to exist.

It is possible to overcome this problem by postulating the existence of jump phenomena [25]. Otherwise, and in an almost equivalent way, impasse points can be broken by inserting a small parasitic capacitance $C$ modeling for instance the electric field between the inductor terminals (Fig. 14(a)). The obtained circuit now has a global SE representation in the $(\varphi, q)$-domain that can be written by inspection as (Fig. 14(b))

$$\begin{aligned} C\dot{\varphi}_C(t;t_0) = {} & -f_M(\varphi_C(t;t_0) + \varphi_{M0}) \\ & + f(\varphi_{M0}) + q_L(t;t_0) + q_{C0} \end{aligned} \tag{31}$$

$$\dot{q}_L(t;t_0) = f_L(-\varphi_C(t;t_0) + \varphi_e(t;t_0) - \varphi_{L0}). \tag{32}$$

The state variables are $\varphi_C(t;t_0)$ and $q_L(t;t_0)$. The existence of the global SE representation rules out in particular the presence of impasse points [19].

The SEs in the $(v, i)$-domain are obtained from the circuit in Fig. 14(a) as

$$\begin{aligned} \dot{\varphi}_M(t) &= \frac{q_C(t)}{C} \\ \dot{q}_C(t) &= -f_M'(\varphi_M(t))\frac{q_C(t)}{C} + f_L(\varphi_L(t)) \end{aligned} \tag{33}$$

$$\dot{\varphi}_L(t) = -\frac{q_C(t)}{C} + e(t). \tag{34}$$

The state variables are $\varphi_M(t), q_C(t), \varphi_L(t)$.

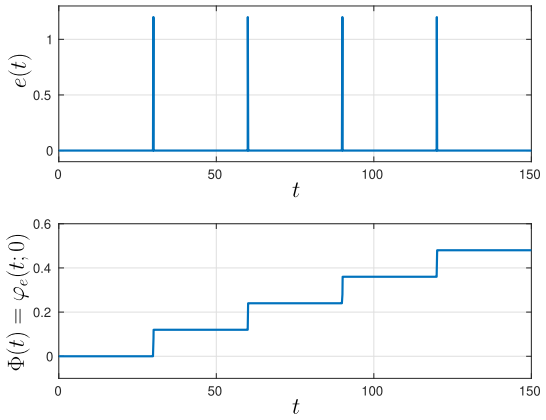


Fig. 15. Input signal $e(\cdot)$ given by a sequence of four short rectangular impulses (upper plot) and time-domain behavior of $\Phi(t) = \varphi_e(t;0) = \int_0^t e(\tau)d\tau$ (lower plot).

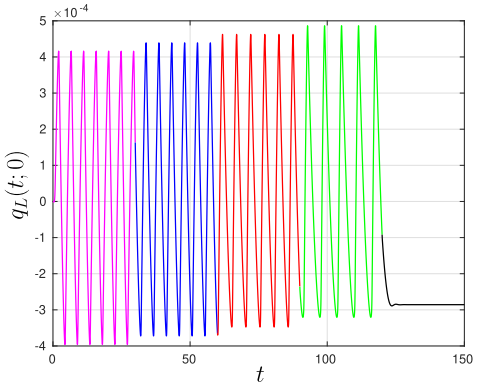


Fig. 16. Time-domain behavior of a solution of the memristor and nonlinear inductor circuit that starts on $\mathcal{M}(0)$ and displays oscillations with almost equal amplitude and increasing period. The solution eventually tends to an equilibrium point.

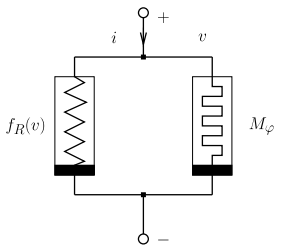


Fig. 17. An extended memristor model of real memristive devices.

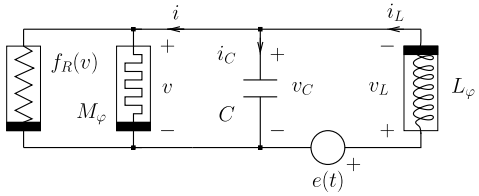


Fig. 18. Relaxation oscillator with an extended memristor model.

These SEs can be obtained also via the method described in Section II. We leave it to the reader to verify this fact and also verify that in this case the hybrid representation is such that $H_{22}$ is singular, hence invariant manifolds cannot be directly obtained via the technique in Section III. Nevertheless, invariant manifolds may be found by noting that from a topological viewpoint the circuit has a loop given by the memristor, inductor and voltage source. Applying K$\varphi$L to this loop, we have $\varphi_M(t;t_0) + \varphi_L(t;t_0) - \varphi_e(t;t_0) = 0$, hence

$$\Phi(t) \doteq \varphi_M(t) + \varphi_L(t) = \varphi_{M0} + \varphi_{L0} - \varphi_e(t;t_0) \qquad (35)$$

for any $t \geq t_0$. Clearly, in the input-less case $\varphi_e(t;t_0) = 0$ for any $t \geq t_0$, we have that each set

$$\mathcal{M}(\Phi_0) = \{(\varphi_M, v_C, \varphi_L)^T \in \mathbb{R}^3 : \varphi_M + \varphi_L = \Phi_0\} \qquad (36)$$

where $\Phi_0 \in \mathbb{R}$, is positively invariant for the dynamics of the circuit in the $(v,i)$-domain. Note that such invariant manifolds are planar, which is different from what has been found in Section III under the assumption that $H_{22}$ is nonsingular.

The input source $e(t)$ $(\varphi_e(t;t_0))$ may be used as for the modified Chua's circuit for steering the dynamics through different manifolds. Suppose the circuit is on manifold $\mathcal{M}(0)$ at $t_0 = 0$ and apply the sequence of four impulses with equal length $\Delta = 0.1$ and area 0.12 as shown in Fig. 15. Due to (35), the impulses cause the circuit solution to pass from manifold $\mathcal{M}(0)$ to manifold $\mathcal{M}(-0.12)$, $\mathcal{M}(-0.24)$, $\mathcal{M}(-0.36)$ and finally to $\mathcal{M}(-0.48)$. We performed computer simulations by choosing $C = 0.0001$, parameters $\alpha = -0.001$, $\beta = 0.005$ for the memristor characteristic and the characteristic in Fig. 12(b) for the nonlinear inductor. It is seen from the simulations in Fig. 16 that the circuit displays oscillations with slightly increasing period and different shape when passing from $\mathcal{M}(0)$ to $\mathcal{M}(-0.36)$. On $\mathcal{M}(-0.48)$ we have instead convergence toward an equilibrium point.

### A. FCAM for Circuits Including an Extended Memristor

A more realistic model of some real memristor devices has been proposed in [26] and consists of the parallel connection of an ideal flux-controlled memristor $q_M = f_M(\varphi_M)$ and a nonlinear resistor $i = f_R(v)$ (Fig. 17), where $f_R(\cdot)$ is a smooth locally Lipschitz function. This corresponds to an extended memristor [27] satisfying the state-dependent Ohm's law

$$i(t) = \left(f'_M(\varphi_M(t)) + \frac{f_R(v(t))}{v(t)}\right) v(t)$$

for any $v(t) \neq 0$, $i(t) = 0$ if $v(t) = 0$, with

$$\frac{d\varphi_M(t)}{dt} = v(t).$$

The nonlinear resistor may account for the junction rectifying effects that are observed in some memristor implementations (cf. [28]). In such a case, $f_R(\cdot)$ has a typical exponential diode-like shape. Although relatively simple, such a model may account for phenomena observed in actual memristor devices as the nonsymmetric loops about the origin of the $v-i$ plane displayed when they are subject to a sinusoidal voltage [26].

Next, we study what happens when inserting such an extended memristor model into the relaxation oscillator previously analyzed (cf. Fig. 18). The SEs in the $(v,i)$-domain are

obtained as

$$\dot{\varphi}_M(t) = \frac{q_C(t)}{C} \tag{37}$$

$$\dot{q}_C(t) = -f'_M(\varphi_M(t))\frac{q_C(t)}{C} - f_R\left(\frac{q_C(t)}{C}\right) + f_L(\varphi_L(t)) \tag{38}$$

$$\dot{\varphi}_L(t) = -\frac{q_C(t)}{C} + e(t). \tag{39}$$

These yield

$$\frac{d\varphi_M(t)}{dt} + \frac{d\varphi_L(t)}{dt} + e(t) = 0$$

hence

$$\varphi_M(t) + \varphi_L(t) = \varphi_{M0} + \varphi_{L0} - \varphi_e(t; t_0) = \Phi_0 - \varphi_e(t; t_0) \tag{40}$$

for any $t \geq t_0$. Hence, in the inputless case $e(t) = 0$, $t \geq t_0$, there exist the same planar invariant manifolds given in (36) as for the circuit with an ideal memristor. This is not surprising, indeed the insertion of the nonlinear resistor $f_R(\cdot)$ does not destroy the loop made by the memristor, the inductor and the voltage source.

From (40), we obtain

$$\varphi_M(t) = -\varphi_L(t) + \Phi_0 - \varphi_e(t; t_0).$$

Then, the circuit satisfies the second-order SE in the $(v, i)$-domain

$$\dot{q}_C(t) = -f'_M(-\varphi_L(t) + \Phi_0 + \varphi_e(t; t_0))\frac{q_C(t)}{C} - f_R\left(\frac{q_C(t)}{C}\right) + f_L(\varphi_L(t)) \tag{41}$$

$$\dot{\varphi}_L(t) = -\frac{q_C(t)}{C} + e(t). \tag{42}$$

We repeated the previous experiment by applying to the circuit with an extended memristor the same sequence of four impulses as in Fig. 15. For the nonlinear resistor we have chosen the characteristic of a Shockley diode

$$i = f_R(v) = I_s\left(e^{\frac{v}{\eta v_T}} - 1\right)$$

with $I_s = 10^{-12}$ A, $v_T = 26 \cdot 10^{-3}$ V and $\eta = 1.7$. The simulation results in Fig. 19 show that once more the circuit displays oscillations with increasing period on the subsequent manifolds visited by the solution. As expected, the effect of the diode is mainly that of reducing in an asymmetric way the amplitude of oscillations on each manifold (compare Fig. 16 with Fig. 19).

*Remark 6:* The article [25] discusses a more realistic model of the nonlinear inductor accounting also for losses. The model is given by a nonlinear inductor (a lossless element) with a characteristic as that in Fig. 12(b), and named restoring function, in parallel to a nonlinear resistor $i = f_{RL}(v)$ (a dissipative element) with a strictly monotone increasing voltage-current characteristic, named dissipation function. There is no additional difficulty in considering such a general model in the circuit in Fig. 18. In fact, once more the nonlinear resistor $f_{RL}$ does not break the loop formed by the (ideal) memristor, the inductor and the voltage source, so that there are still planar invariant manifolds as in (36) and there is also a reduction of order for the dynamics on invariant manifolds. A detailed treatment is omitted for brevity.

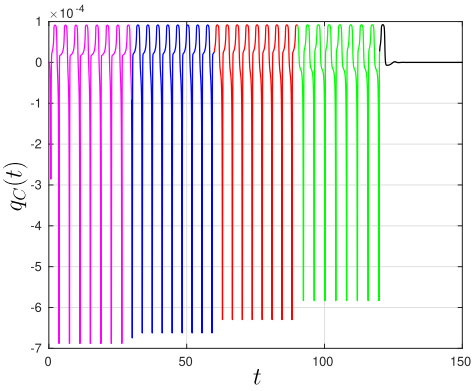


Fig. 19. Time-domain behavior of a solution of the extended memristor and nonlinear inductor circuit.

## VI. Conclusion

The SE representation in the $(\varphi, q)$-domain and $(v, i)$-domain, in combination with an extension of the FCAM theory in [14]–[16], have been proved effective to unfold the dynamics of a class of memristor circuits with nonlinear storage elements. In particular, we have shown that a modified Chua's circuit with a memristor and a nonlinear capacitor displays a rich dynamic scenario including the coexistence of different regimes (periodic, chaotic) and period-doubling bifurcations due to changing the initial conditions for a fixed set of circuit parameters (bifurcations without parameters). In a second example, we have shown that the peculiar phenomena of coexistence of different attractors, as equilibria and limit cycles, is displayed also by a relaxation oscillator with a memristor and a nonlinear inductor. In both cases, pulse current or voltage sources can be designed to steer trajectories through different manifolds and dynamics. These results show that such kind of circuits are a source of programmable complex dynamics that can be implemented at nanoscale and are potentially useful for incorporation in future neuromorphic computing systems.

## References

[1] R. S. Williams, "What's next? [The end of Moore's law]," *Comput. Sci. Eng.*, vol. 19, no. 2, pp. 7–13, Mar./Apr. 2017.

[2] M. A. Zidan, J. P. Strachan, and W. D. Lu, "The future of electronics based on memristive systems," *Nature Electron.*, vol. 1, no. 1, p. 22, Jan. 2018.

[3] D. Ielmini and H.-S.-P. Wong, "In-memory computing with resistive switching devices," *Nature Electron.*, vol. 1, no. 6, pp. 333–343, Jun. 2018.

[4] F. Corinto, M. Di Marco, M. Forti, and L. Chua, "Nonlinear networks with Mem-elements: Complex dynamics via flux-charge analysis method," *IEEE Trans. Cybern.*, early access, Apr. 3, 2019, doi: 10.1109/TCYB.2019.2904903.

[5] S. R. Nandakumar, S. R. Kulkarni, A. V. Babu, and B. Rajendran, "Building brain-inspired computing systems: Examining the role of nanoscale devices," *IEEE Nanotechnol. Mag.*, vol. 12, no. 3, pp. 19–35, Sep. 2018.
[6] C. Li *et al.*, "Long short-term memory networks in memristor crossbar arrays," *Nature Mach. Intell.*, vol. 1, no. 1, pp. 49–57, 2019.
[7] M. Itoh and L. O. Chua, "Memristor oscillators," *Int. J. Bifurcation Chaos*, vol. 18, no. 11, pp. 3183–3206, Nov. 2008.
[8] F. Corinto, A. Ascoli, and M. Gilli, "Nonlinear dynamics of memristor oscillators," *IEEE Trans. Circuits Syst. I, Reg. Papers*, vol. 58, no. 6, pp. 1323–1336, Jun. 2011.
[9] M. D. C. Scarabello and M. Messias, "Bifurcations leading to nonlinear oscillations in a 3D piecewise linear memristor oscillator," *Int. J. Bifurcation Chaos*, vol. 24, no. 01, Jan. 2014, Art. no. 1430001.
[10] R. Riaza, "Manifolds of equilibria and bifurcations without parameters in memristive circuits," *SIAM J. Appl. Math.*, vol. 72, no. 3, pp. 877–896, Jan. 2012.
[11] R. Tetzlaff, A. Ascoli, I. Messaris, and L. O. Chua, "Theoretical foundations of memristor cellular nonlinear networks: Memcomputing with bistable-like memristors," *IEEE Trans. Circuits Syst. I, Reg. Papers*, vol. 67, no. 2, pp. 502–515, Feb. 2020.
[12] A. Ascoli, I. Messaris, R. Tetzlaff, and L. O. Chua, "Theoretical foundations of memristor cellular nonlinear networks: Stability analysis with dynamic memristors," *IEEE Trans. Circuits Syst. I, Reg. Papers*, vol. 67, no. 4, pp. 1389–1401, Apr. 2020.
[13] A. Ascoli, S. Slesazeck, H. Mahne, R. Tetzlaff, and T. Mikolajick, "Nonlinear dynamics of a locally-active memristor," *IEEE Trans. Circuits Syst. I, Reg. Papers*, vol. 62, no. 4, pp. 1165–1174, Apr. 2015.
[14] F. Corinto and M. Forti, "Memristor circuits: Flux—Charge analysis method," *IEEE Trans. Circuits Syst. I, Reg. Papers*, vol. 63, no. 11, pp. 1997–2009, Nov. 2016.
[15] F. Corinto and M. Forti, "Memristor circuits: Bifurcations without parameters," *IEEE Trans. Circuits Syst. I, Reg. Papers*, vol. 64, no. 6, pp. 1540–1551, Jun. 2017.
[16] F. Corinto and M. Forti, "Memristor circuits: Pulse programming via invariant manifolds," *IEEE Trans. Circuits Syst. I, Reg. Papers*, vol. 65, no. 4, pp. 1327–1339, Apr. 2018.
[17] L. O. Chua, "Nonlinear circuit foundations for nanodevices. I. The four-element torus," *Proc. IEEE*, vol. 91, no. 11, pp. 1830–1859, Nov. 2003.
[18] M. Di Marco, M. Forti, F. Corinto, and M. Gilli, "State equations of memristor circuits with nonlinear lossless elements in the flux-charge domain," in *Proc. IEEE Int. Symp. Circuits Syst. (ISCAS)*, May 2019, pp. 1–5.
[19] L. Chua, "Dynamic nonlinear networks: State-of-the-art," *IEEE Trans. Circuits Syst.*, vol. 27, no. 11, pp. 1059–1087, Nov. 1980.
[20] L. O. Chua, C. A. Desoer, and E. S. Kuh, *Linear and Nonlinear Circuits*. New York, NY, USA: McGraw-Hill, 1987.
[21] R. M. Corless, "What good are numerical simulations of chaotic dynamical systems?" *Comput. Math. with Appl.*, vol. 28, nos. 10–12, pp. 107–121, Nov. 1994.
[22] E. G. Nepomuceno, S. A. M. Martins, B. C. Silva, G. F. V. Amaral, and M. Perc, "Detecting unreliable computer simulations of recursive functions with interval extensions," *Appl. Math. Comput.*, vol. 329, pp. 408–419, Jul. 2018.
[23] H. Bao, N. Wang, B. Bao, M. Chen, P. Jin, and G. Wang, "Initial condition-dependent dynamics and transient period in memristor-based hypogenetic jerk system with four line equilibria," *Commun. Nonlinear Sci. Numer. Simul.*, vol. 57, pp. 264–275, Apr. 2018.
[24] H. Chang, Y. Li, F. Yuan, and G. Chen, "Extreme multistability with hidden attractors in a simplest memristor-based circuit," *Int. J. Bifurcation Chaos*, vol. 29, no. 06, Jun. 2019, Art. no. 1950086.
[25] L. Chua and K. Stromsmoe, "Lumped-circuit models for nonlinear inductors exhibiting hysteresis loops," *IEEE Trans. Circuit Theory*, vol. 17, no. 4, pp. 564–574, Nov. 1970.
[26] F. Corinto, M. Gilli, and M. Forti, "Flux-charge description of circuits with non-volatile switching memristor devices," *IEEE Trans. Circuits Syst. II, Exp. Briefs*, vol. 65, no. 5, pp. 642–646, May 2018.
[27] L. Chua, "Everything you wish to know about memristors but are afraid to ask," *Radioengineering*, vol. 24, no. 2, pp. 319–368, Jun. 2015.
[28] J. J. Yang, M. D. Pickett, X. Li, D. A. A. Ohlberg, D. R. Stewart, and R. S. Williams, "Memristive switching mechanism for metal/oxide/metal nanodevices," *Nature Nanotechnol.*, vol. 3, no. 7, pp. 429–433, 2008.

**Mauro Di Marco** was born in Firenze, Italy, in 1970. He received the Laurea degree in electronic engineering from the University of Firenze, Firenze, Italy, in 1997, and the Ph.D. degree from the University of Bologna, Bologna, Italy, in 2001. From November 1999 to April 2000, he held a Visiting Researcher position at LAAS, Toulouse, France. Since 2000, he has been with the University of Siena, Siena, Italy, where he is currently an Associate Professor of circuit theory. He is the author of more than 80 technical publications. His current research interests include analysis and modeling of nonlinear dynamics of complex systems and neural and robust estimation and filtering. From 2007 to 2011, he was serving as an Associate Editor for the IEEE TRANSACTIONS ON CIRCUITS AND SYSTEMS—I: REGULAR PAPERS.

**Mauro Forti** received the Laurea degree in electronics engineering from the University of Florence, Italy, in 1988. From 1991 to 1998, he was an Assistant Professor of applied mathematics and network theory with the Department of Electronic Engineering, University of Florence. In 1998, he joined the Department of Information Engineering and Mathematics, University of Siena, Italy, where he is currently a Professor of electrical engineering. His research interests include nonlinear circuits and systems, with an emphasis on the qualitative analysis and stability of circuits modeling artificial neural networks, and aspects of electromagnetic compatibility. He has served as an Associate Editor for the IEEE TRANSACTIONS ON CIRCUITS AND SYSTEMS—I: FUNDAMENTAL THEORY AND APPLICATIONS from 2001 to 2003 and the IEEE TRANSACTIONS ON NEURAL NETWORKS from 2001 to 2010. He is also serving as an Associate Editor for the IEEE TRANSACTIONS ON CYBERNETICS and *Neural Networks*.

**Fernando Corinto** (Senior Member, IEEE) received the master's degree in electronic engineering and the Ph.D. degree in electronics and communications engineering from the Politecnico di Torino, in 2001 and 2005, respectively. He also received the European Doctorate from the Politecnico di Torino, in 2005. He is currently a Professor of electrical engineering with the Department of Electronics and Telecommunications, Politecnico di Torino. He is the coauthor of one book, eight book chapters, and more than 150 international journal and conference papers. His research interests include nonlinear circuits and systems, locally coupled nonlinear/nanoscale networks, and memristor nanotechnology. He is also a member of the Institute for Advanced Study, Technische Universitat Munchen. He was awarded a Marie Curie Fellowship in 2004. He was the Vice Chair of the COST Action: Memristors-Devices, Models, Circuits, Systems and Applications (MemoCiS). He was a DRESDEN Senior Fellow with the Technische Universitat Dresden in 2013 and 2017. He was also an August–Wilhelm Scheer Visiting Professor, Technische Universitat Munchen, in 2016, and an Associate Editor of the IEEE TRANSACTION ON CIRCUITS AND SYSTEMS—I: REGULAR PAPERS from 2014 to 2015. He has been on the Editorial Board and a Review Editor of the *International Journal of Circuit Theory and Applications* since January 2015.

**Leon Chua** (Life Fellow, IEEE) received the M.S. degree from the Massachusetts Institute of Technology, Cambridge, MA, USA, in 1961, and the Ph.D. degree in electrical engineering from the University of Illinois at Urbana-Champaign, Champaign, IL, USA, in 1964. He has been a Professor with the University of California, Berkeley, Berkeley, CA, USA, since 1971. In 2011, he was appointed as a Distinguished Professor with the Technical University of Münich. He was awarded seven patents and 14 honorary doctorates. When not immersed in science, he relaxes by searching for Wagner's leitmotifs, musing over Kandinsky's chaos, and contemplating Wittgenstein's inner thoughts. He received many awards, including the first recipient of the Gustav Kirchhoff Award, the Guggenheim Fellow Award, and the European EC Marie Curie Fellow Award. He was elected a Foreign Member of the Academia Europaea and the Hungarian Academy of the Sciences. He was elected the Confrérie des Chevaliers du Tastevin in 2000.